International Forum on Aeroelasticity and Structural Dynamics
IFASD 2017
25-28 June 2017 Como, Italy

INDIVIDUAL BLADE REPETITIVE CONTROL FOR HORIZONTAL-AXIS WIND TURBINES

Riccardo Fratini[1], Jacopo Serafini[1], Massimo Gennaretti[1], Riccardo Santini[1], Stefano Panzieri[1]

[1]Department of Engineering
University Roma Tre
via della Vasca Navale, 79 Roma 00146 Italy
riccardo.fratini@uniroma3.it
serafini@uniroma3.it
m.gennaretti@uniroma3.it
riccardo.santini@uniroma3.it
stefano.panzieri@uniroma3.it

Keywords: Control, Repetitive, structural dynamics, aeroelasticity

Abstract: Horizontal axis wind turbine (HAWT) control is crucial for both increasing performance (quantity and quality of power harvested) and avoiding excessive stress of structural components. Indeed, both wind and corresponding torque are time-varying. In particular, boundary conditions over turbine blades are strongly affected by terrain boundary layer, which causes periodic inputs and then vibratory loads. In uncontrolled blades, high vibratory level might arise, along with reduction of generated power. The most effective and multipurpose way to control horizontal axis wind turbine is changing blade pitch in order to guarantee suited aerodynamic incidence, while other control strategies (as yaw or torque control) are mainly aimed at avoiding excessive rotational speed. Acting on blade pitch allows to reduce vibratory loads and regulate generated torque at the same time. In this work, this control approach is described, developed and validated by application to a lumped elasticity pylon/turbine system model.

1 INTRODUCTION

One of the fundamental goal of the wind energy industry is the reduction of the cost of the energy production, to make it competitive with respect to other sources, such as fossil fuels. In the last years, several companies entered the global market, introducing price competitive and high performances wind turbines, resulting in a downward pressure on energy prices. These trends, combined with overcapacity of the wind turbine manufacturers, drive the price per installed MW power down drastically [1]. Even though the customers benefit from this aspect, on the other hand, the manufacturers experienced increasingly competition to retain their market share. As a result, the need of increasingly performing HAWT is one of the crucial aspect that have led to close collaboration between academia and industry. Nowadays, two trends can be identified in turbine design: turbines are getting larger both in terms of power extracted and rotor diameter, leading to a shift towards offshore wind turbines.

As the turbines get larger, the rotor area increases, the wake vorticity becomes stronger, the tower shadow is larger because of the larger tower that carries the heavier nacelle and rotor, and the wind shear increases giving stronger vibratory loads [2–6]. Another important aspect related

to the increasing dimension of the rotor disc is the weight of the disc itself. This effect can be determined by observing some basic scaling laws: the power output raises with the square of the scale factor, whereas the weight generally increases with the third power. Having wind turbines to operate over a design life of 20 years or more, the analysis of the effects of the loads acting on the structure in different operating conditions is mandatory. The mechanical loads can be divided into two categories: the static ones, which are the result of interaction between the turbine and mean wind velocity, and the dynamic ones, which are induced by spatial and temporal non-uniform distribution of wind velocity within the area swept by the rotor. Dynamic loads are also present in the form of transient loads (low frequency), caused by turbulence and gusts, or cyclic loads that are related to the interaction between asymmetric loads or external disturbances with the wind turbine structure. In addition to unsteady wind effects (wind shear, gust, turbulence), the HAWT experiences several negative effects as a result of a pitch change imposed by the controller to match the optimal operational point: blade vibrations, material fatigue, peak forces and blade stall are the most important ones [7]. At the same time, the vibratory loads affecting the mechanical parts can be reduced controlling the pitch angle in order to extend their life time.

For wind turbines control, three actuation strategies are usually applicable: blade pitch, generator torque, and machine yaw [8], [9], [10], [11] that can be used in different operational conditions, depending on wind speed magnitude. Usually, the turbine starts producing electricity at a wind velocity of 3-5 m/s, also called the cut-in wind speed, shuts down at approximately 25 m/s, also called the cut-out wind speed and reaches its nominal, or rated wind speed, at around 11-14 m/s. We can divide wind speed range into two main parts: the region between the cut-in wind speed and nominal wind speed is called region 1 and the blades are set at an optimal pitch angle, whereas the region up to cut-out wind speed is called region 3. Advanced control techniques have been studied extensively for energy capture in region 1 and load reduction for region 3 operations, in order to reduce the cost of energy. The generator torque is most often used in region 1 to maintain turbine operation at maximum power coefficient, C_p. It can also be used to add damping to the drive-train torsion modes of the turbine in region 3. In addition, the turbine power output can be limited by yawing the machine out of the wind, thereby decreasing the projected rotor area and reducing power. Most often, yaw control is used only to respond to changes in wind direction in the attempt to reduce the yaw error (the angle between the mean wind direction and the direction of orientation of the turbine) and thereby maximize power. The blade pitch controller, instead, is the most effective device to control aerodynamic loads. There are two types of this controller: Collective Pitch Control (CPC) and Individual Pitch Control (IPC). The main differences lie on the control commands: for the CPC the blades are pitched using a common (collective) signal, whereas for the IPC each blade is pitched independently of the others.

A major drawback of CPC is the inability of dealing with asymmetric load [12]. Several IPC schemes have been developed to deal with the asymmetric loads of turbine [13], [14], [15] [16] [17] [18] [19], considering different measurement setup: strain gauge sensors installed at the blade root, measurement of the nacelle tilt and yawing moment, of the drive-train shaft bending moments or of acceleration of the rotor blade tips and local blade wind inflow measurements. Individual pitch control and field tests to assess the viability of such strategy are studied, for instance, in [20], [12]. In [21] a multiple model robust control strategy is considered, and a fault tolerant pitch control is proposed to rejects faults in a turbine pitch actuator. Moreover, model predictive control (MPC) techniques are active research topics in this field and recent studies have shown promising results [22], [23], [24]. Finally, repetitive control strategies for

wind turbines have been proposed in [24], [25], [26], [27] when the reference command to be tracked and/or the disturbance to be rejected are periodic signals with a fixed period.

In this paper, with the aim of reducing the vibratory loads generated in periodic operating conditions while maintaining the turbine rotational speed, the authors propose the application of repetitive control to IPC. Indeed, when the reference command to be tracked and/or the disturbance to be eliminated are periodic signals, the repetitive control strategy may be successfully applied due to its precision, ease of implementation and performance weakly dependent on system parameters. Much attention is paid on fatigue loads due to incident wind variation along the span blade and height (see Figs. (1,4)). Blade root flapping moment introduce yawing and tilting moments which are transmitted through the drive train to the yaw system and the tower. This can lead to damages of turbine components and eventually failures [5]. Here the Repetitive IPC is applied on a 5 MW horizontal axis wind turbine. Firstly, a mid-fidelity nonlinear differential model for a three-bladed HAWT wind turbine is outlined and the influence of wind shear on wind turbine dynamics is described. Secondly, a *spatial* repetitive control algorithm is proposed in order to reject periodic model dynamics responses both through collective and individual actuation.

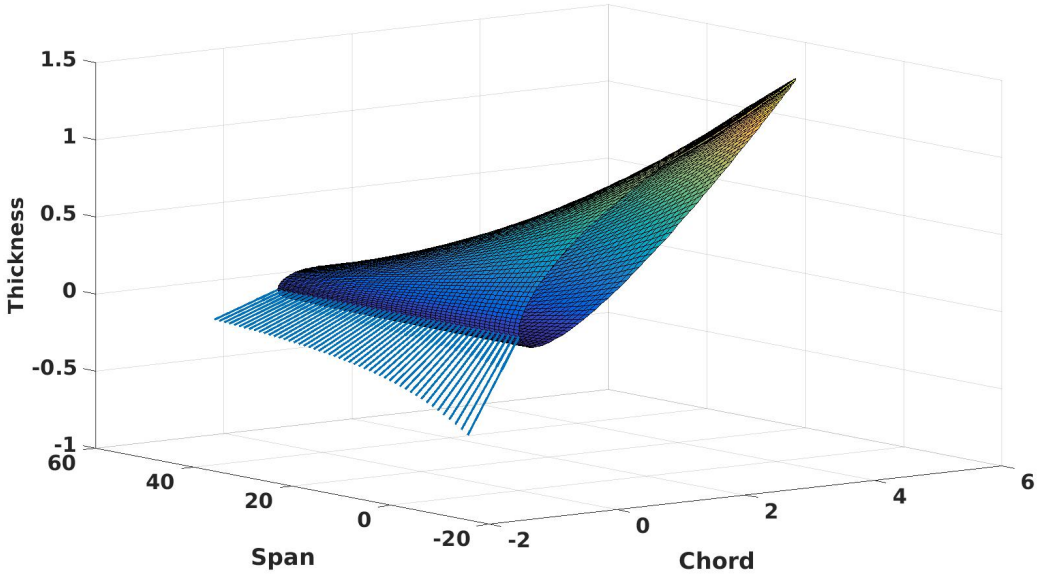

Figure 1: Incidence variation along span.

2 AEROELASTIC MODEL

The aerodynamic forces applied on the blades of a turbine are produced by interaction with the wind and are such to produce rotor angular velocity. This is obtained by the torque load that, through a low pass speed shaft, is transmitted to the gearbox that is connected to the generator by a high speed shaft. The aerodynamic loads acting on the rotor, in addition to providing the torque driving the generator, force the wind turbine structure, thus inducing structural displacements of tower and blades. In particular, the thrust force is responsible for tower deformation, while blade distributed loads generate flap-wise blade bending. In turn, these displacements affect the aerodynamic field and hence the rotor loads, thus yielding the aeroelastic loop to be considered for a suitable simulation of HAWT energy harvesting.

Here, the aeroelastic model of a HAWT to be controlled (aero-servo-elastic model) is derived by moving from the Euler-Lagrange differential equations applied to a lumped-parameter description of the tower-rotor system (*Energetic Variational Approach*). Kinetic energy, $\mathcal{T} = \mathcal{T}(\dot{\mathbf{q}}, \mathbf{q})$, and potential energy, $\mathcal{U} = \mathcal{U}(\mathbf{q})$, are defined as functions of the Lagrangean coordinates, $\mathbf{q}$ including rigid and elastic system dofs. The aerodynamic loads contribute as generalized forces $F_i = F_i(\ddot{\mathbf{q}}, \dot{\mathbf{q}}, \mathbf{q})$. The aero-servo-elastic model developed considers eight dofs, namely, $q_1 = z_p$, $q_{2,3,4} = \beta_{1,2,3}$, $q_{5,6,7} = \theta_{1,2,3}$, $q_8 = \Psi$, where z_p represents the tower fore-aft elastic motion, β and θ are, respectively, flap and pitch angle of the three blades composing the rotor (assumed to be rigid bodies), and Ψ denotes the azimuthal position of the rotor.

The following nonlinear differential set of equations is derived:

$$
\begin{aligned}
& m_{tot}\ddot{z}_p - \sum_{i=1}^{3} m_b x_{g_b} \ddot{\beta}_i^2 + k_p z_p \; = \sum_{i=1}^{3} \int_0^L L_{w_i} dr \\
& J_{o_y}\ddot{\beta}_1 - m_b x_{g_b}\ddot{z}_p + \left(J_{o_y}\Omega^2 + m_b x_{g_b} f\Omega^2 + k_{\beta_1}\right)\beta_1 - m_b x_{g_b} g \sin\Psi_1 - J_{g_x}\dot{\Omega}\theta_1 = \int_0^L L_{w_1} r dr \\
& J_{o_y}\ddot{\beta}_2 - m_b x_{g_b}\ddot{z}_p + \left(J_{o_y}\Omega^2 + m_b x_{g_b} f\Omega^2 + k_{\beta_2}\right)\beta_2 - m_b x_{g_b} g \sin\Psi_2 - J_{g_x}\dot{\Omega}\theta_2 = \int_0^L L_{w_2} r dr \\
& J_{o_y}\ddot{\beta}_3 - m_b x_{g_b}\ddot{z}_p + \left(J_{o_y}\Omega^2 + m_b x_{g_b} f\Omega^2 + k_{\beta_3}\right)\beta_3 - m_b x_{g_b} g \sin\Psi_3 - J_{g_x}\dot{\Omega}\theta_3 = \int_0^L L_{w_3} r dr \\
& \sum_{i=1}^{3}\left[m_b f^2 + J_{o_z} + 2 m_b x_{g_b} f\right]\dot{\Omega} - 2\sum_{i=1}^{3} J_{o_y}\Omega\dot{\beta}_i\beta_i = \sum_{i=1}^{3}\int_0^L L_{v_i}(r+f) dr \\
& J_{g_x}\dot{\theta}_1 + J_{g_x}\Omega^2\theta_1 - J_{g_x}\beta_1\dot{\Omega} = \int_0^L M_{\phi_2} dr + C_{c_1} \\
& J_{g_x}\dot{\theta}_2 + J_{g_x}\Omega^2\theta_2 - J_{g_x}\beta_2\dot{\Omega} = \int_0^L M_{\phi_2} dr + C_{c_2} \\
& J_{g_x}\dot{\theta}_3 + J_{g_x}\Omega^2\theta_3 - J_{g_x}\beta_3\dot{\Omega} = \int_0^L M_{\phi_3} dr + C_{c_3}
\end{aligned}
\tag{1}
$$

where $\Omega = \dot{\psi}$ is the rotor angular velocity, f is the distance between flapping hinge and rotation axis, and g is the gravitational acceleration.

2.1 Aerodynamic loads

Aerodynamic loads are determined by the quasi-steady approximation of the Greenberg theory [28], for which the lift deficiency function is assumed to be equal to 1 (it can be observed that this imply there is no phase delay between body motion and corresponding aerodynamic loads [29]). These are composed of a circulatory component due to the circulation around the airfoil and a non-circulatory components deriving from unsteady motion effects (regardless the presence of circulation). Furthermore, a simple expression for drag is added through inclusion of the drag coefficient, C_{d0}.

Following the approach proposed by Hodges and Ormiston [30], the aerodynamic loads are expressed as functions of the chord-wise and normal components of the relative velocity between flow and airfoil at the quarter-chord point, and of the section angular velocity. Thus, the following expressions for in-plane (L_v) and out-of-plane (L_w) sectional forces and moment (M_ψ) are

obtained [30] (see Fig. 2):

$$
\begin{aligned}
L_v \approx & \frac{2\pi\rho c}{2}\Big[V_w(V_w-\Omega r\theta)(S^2\phi\, C\phi + C^3\phi) - \frac{C_{d_0}\Omega^2 r^2 C^3\phi}{2\pi} \\
& -\Omega r\big(r\dot{\beta}+V_w-\dot{z}_p\big)(S\phi\, C^2\phi + S^3\phi) - \frac{c}{4}\dot{\Omega} r\, S^2\phi\Big]
\end{aligned}
$$

$$
\begin{aligned}
L_w \approx & \frac{2\pi\rho c}{2}\Big[\Omega^2 r(r+2f)(S\phi\, C^2\phi + S^3\phi) - \frac{C_{d_0}\Omega^2 r^2\, S\phi\, C^2\phi}{2\pi} \\
& +\Omega r(\dot{z}_p+\Omega r\theta - V_w - r\dot{\beta})(S^2\phi C\phi + C^3\phi) + \frac{c}{4}\dot{\Omega} r S\phi C\phi + 2\Omega r f\, S\phi\, C^2\phi\Big]
\end{aligned}
\tag{2}
$$

$$
M_\phi \approx -\frac{2\pi\rho c}{2}\left(\frac{c}{4}\right)^2\Big[\dot{\Omega}(r+f)S\phi + (\Omega^2 r\beta + \ddot{z}_p + \dot{\Omega} r\theta + 2\Omega r\dot{\theta} - \ddot{\beta} r - V_w C\phi)\Big]
$$

where c is the blade chord, ρ is the air density, V_w is the wind velocity, ϕ is the blade geometric twist, whereas S and C are abbreviation for $\sin()$ and $\cos()$.

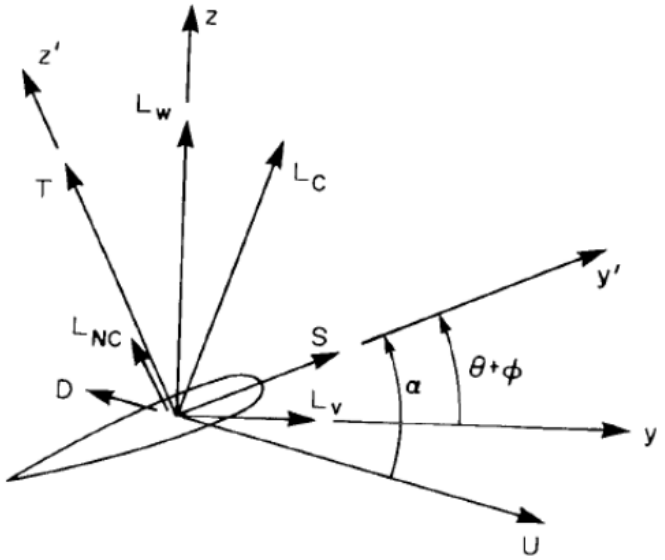

Figure 2: Section velocity, from [30].

3 CONTROL OBJECTIVES AND STRATEGIES

In this section, objective and strategies for the wind turbines control are outlined. In particular, the repetitive control strategy is introduced and a spatial repetitive controller algorithm is proposed. In the operational region 3, the control is often based on pitch actuation, with the aim of searching the optimal pitch angle with respect to the wind velocity, such to provide the objective nominal rotor speed suitable for optimal HAWT performance.

When a vertical wind shear is present, each blade section experiences a different relative wind that changes local angle of attack and dynamic pressure. Moving from the bottom to the top of the rotor disc, the aerodynamic loads change, thereby generating periodic flapping motion, with oscillations that are increased with respect to the constant wind case (see Fig. 5). These oscillations are coupled with vibratory loads that should be alleviated by the controller actuation.

In this work, a repetitive control strategy is applied to the model proposed, in such way that once a specific undesired system "behavior" is learned, the controller is capable to reject it. The basis of the approach is the linear iterative learning control theory:

$$y_j(k) = P(q)u_j(k) + d(k) \tag{3}$$

where k is the time index, j is the iteration index, q is the forward time-shift operator such that $qx(k)x(k+1)$, y_j is the output, u_j is the control input, and d is an exogenous signal that repeats each iteration. The plant $P(q)$ is a proper function of q with delay. In what follows, the N-sample sequence of inputs and outputs are reported:

$$u_j(k), k \in \{0, 1, ..., N-1\},$$
$$y_j(k), k \in \{0, 1, ..., N-1\},$$
$$d_j(k), k \in \{0, 1, ..., N-1\}.$$

The desired output reads as:

$$y_d(k), k \in \{0, 1, ..., N-1\}.$$

The system error signal is defined by :

$$e_j(k) = y_d(k) - y_j(k).$$

The N-sample sequence is proportional to the simulation sample time Δt, such that the total simulation time is $T = N\Delta t$.

Now, consider the following discrete dynamical system

$$x_j(k+1) = Ax_j(k) + Bu_j(k) \tag{4}$$
$$y_j(k) = Cx_j(k), \tag{5}$$

where denotes the system matrix, and B contains the torque pitch control input; the corresponding state space representation reads

$$y_j(k) = \underbrace{C(qI - A)^{-1}B}_{P(q)} u_j(k) + \underbrace{CA^k x_0}_{d(k)} \tag{6}$$

where the last term is the free response of the system to the initial condition x_0. A widely used ILC learning algorithm is:

$$u_{j+1}(k) = Q(q)[u_j(k) + L(q)e_j(k+1)] \tag{7}$$

where the LTI dynamics $Q(q)$ and $L(q)$ are defined as the Q-filter and the learning function, respectively. In Fig. 3 the action of the repetitive approach is shown. The control core consists in acquiring control and error signals relative to previous iteration. Then by comparing the two signals for each sample time, control action, for the same sample time at the present iteration, has been synthesized. Two type of graphics are reported, corresponding to control and error signal stories with respect to the iterations j and sample time k. Following Eq. (7) the command input $u_{j+1}(k)$ (related to $j+1$ iteration at sample time k) is proportionally through Q filter to previous command ($u_j(k)$) and error ($e_j(k+1)$), specifically the last one is modulated and shifted through L action. The design of ILC control systems pass through the synthesis of $Q(q)$ and $L(q)$ filters.

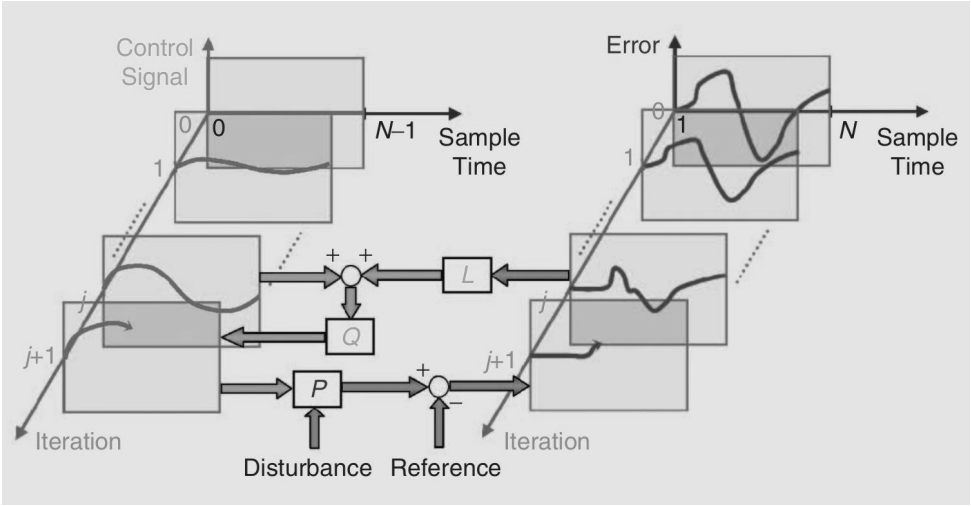

Figure 3: Iterative Learning Control scheme.

4 NUMERICAL RESULTS

In this work, a 5 MW, three-bladed HAWT is examined. It has radius $R = 61.5$ m, mean chord $c = 3$ m, up-wind rotor orientation, hub height from terrain $h = 90$ m, nominal angular speed $\Omega = 1.26$ rad/s, nominal wind speed $V_{wind} = 11.4$ m/s.

If a non-uniform inflow is considered (*e.g.*, due to terrain boundary layer), then periodic aeroelastic inputs and outputs arise. Although wind is usually perceived as a uniform phenomenon with occasional gusts, its nature is essentially dynamic. In general, the derivation of wind profile might be a complex task taking into account wind shear, tower shadowing effects, presence of turbulence and wakes from other HAWTs (if present). In this work, the attention is focused on wind shear, that describes the vertical profile of wind speed. Broadly speaking, it is assumed that the wind speed is low at the Earth's surface and increases with the height. The wind shear is an important factor affecting both energy harvesting performance and aeroelastic response of the wind turbine. Optimal hub height, as well as turbine fatigue loading depend on it. Wind shear is influenced by the surface roughness of the Earths surface and atmospheric stability.

Typically, two types of formula are used to describe wind shear, respectively known as the log-law and the power-law. The log-law describes wind shear through a logarithmic relation dependent on the surface roughness length of the wind site (usually, this parameter is defined empirically). The power-law approach is based on the knowledge of the average wind speed at a reference height and reads

$$U(z) = U(z_r)(\frac{z}{z_r})^{\alpha} \tag{8}$$

where $U(z)$ and $U(z_r)$ are, respectively, the average wind speed in axial direction at height z and at reference height z_r, whereas α is an empirical coefficient that can be determined through fit of wind data. Fig. 4 shows the influence of α on the wind vertical variation, for $U(z_r) = 11.4$ m/s and $z_r = 90$ m.

In this work, it has been assumed $\alpha = 0.17$, thus considering wind speed variation from a minimum value of about 9 m/s to a maximum value of about 12 m/s. As already mentioned, such non-uniform wind distribution causes vibratory loads at the HAWT hub: in the following, individual pitch control based on repetitive control strategy is applied to alleviate such fatigue loadings, while maintaining nominal rotational speed.

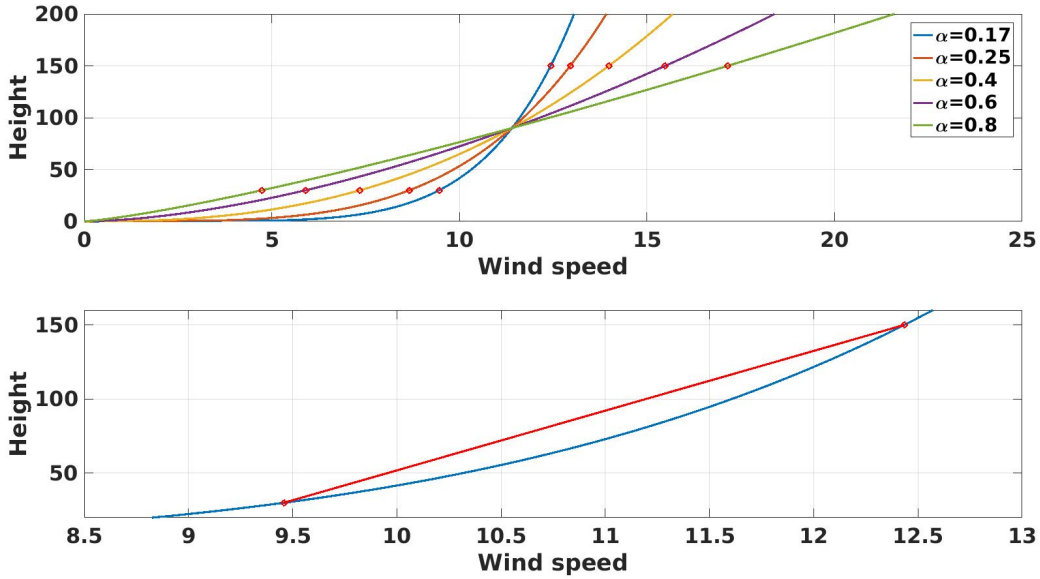

Figure 4: Different wind shear profiles.

First of all the open-loop configuration is analyzed, comparing the aeroelastic response with and without wind shear, starting from the same initial conditions. Figure 5 shows that the wind shear causes a significant increase of flapping response oscillations and associated hub loads (in the absence of wind shear, small-amplitude oscillations appear due to gravity effects). However, small oscillations appear also in the angular velocity response (not shown here) that, in principle, imply undesired oscillations of the output electric power.

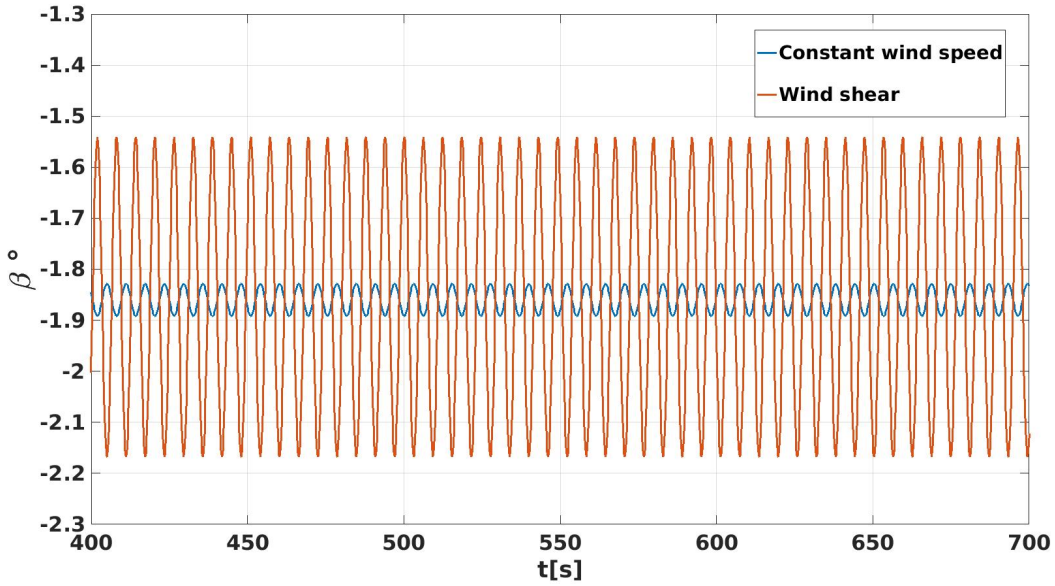

Figure 5: Increase of flapping oscillation amplitude due to wind shear.

Next, the repetitive control is applied separately to both problems, namely angular velocity tracking and vibratory loads alleviation. First, the application of collective repetitive control

(sketched in Fig. 6) to the nominal angular velocity tracking in presence of wind shear and hence periodic wind speed in the rotating frame is discussed. The input $u_j(k)$ is the collective

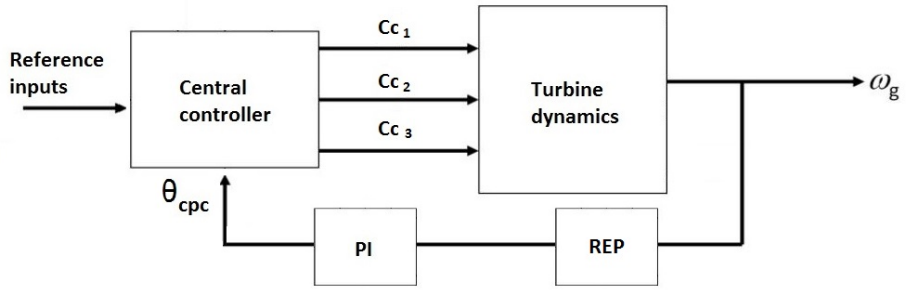

Figure 6: CPC angular velocity control scheme.

torque forcing the pitch dynamics defined in Eq. 1. Moreover, $Q(q)$ is assumed to be an identity matrix and a heuristic approach is followed for the determination of the $L(q)$ filter. In particular, considering $L(q)$ as a function of the gain parameter, G, and of the sample phase shift factor, δ, several tests are performed by varying δ for fixed G. The results show that, for the three values of G considered (namely, $G = 0.5, 1, 1.5$), the lowest tracking error is achieved for $\delta = 120$ samples, as shown in Figs. 7, 8 and 9. Then, fixing this value, the gain parameter is changed. Figure 10 shows that the optimal control configuration is achieved when $G = 1.5$.

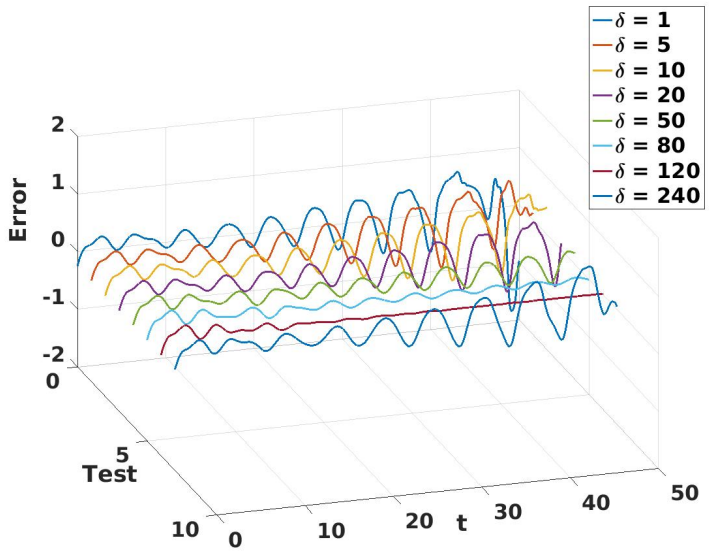

Figure 7: Tuning δ for G = 1.

To test the control algorithm effectiveness, four different simulations with the CPC approach, are performed with inclusion of external periodic disturbances on $U(z_r)$ with frequency equal to $1/rev$, $2/rev$, $3/rev$, $4/rev$ (the fundamental $1/rev$ coincides with the nominal value of the angular velocity). Figures 11,12,13,14 demonstrate that the periodic external disturbances affect the open-loop responses causing significant oscillations of the angular velocity. In addition, the comparison between the results obtained by the proposed repetitive control approach and those from a classical PI approach reveal that the best tracking is obtained by the repetitive controller,

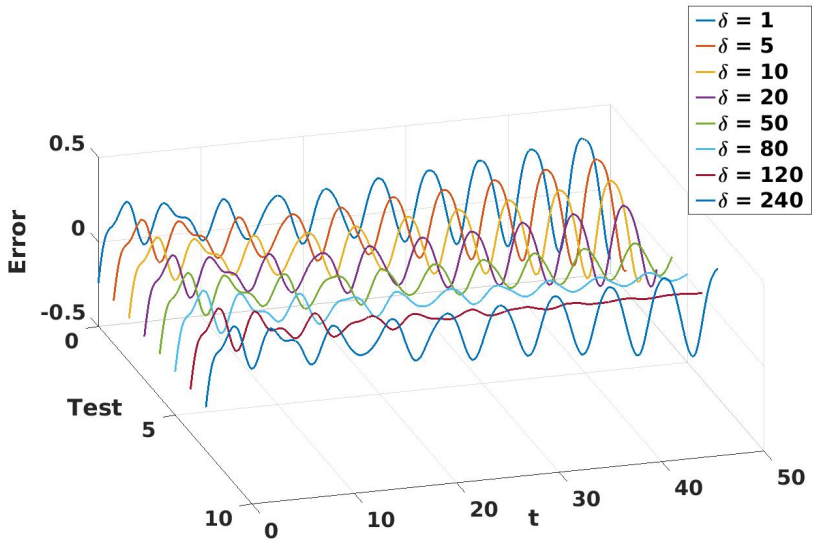

Figure 8: Tuning δ for G = 0.5.

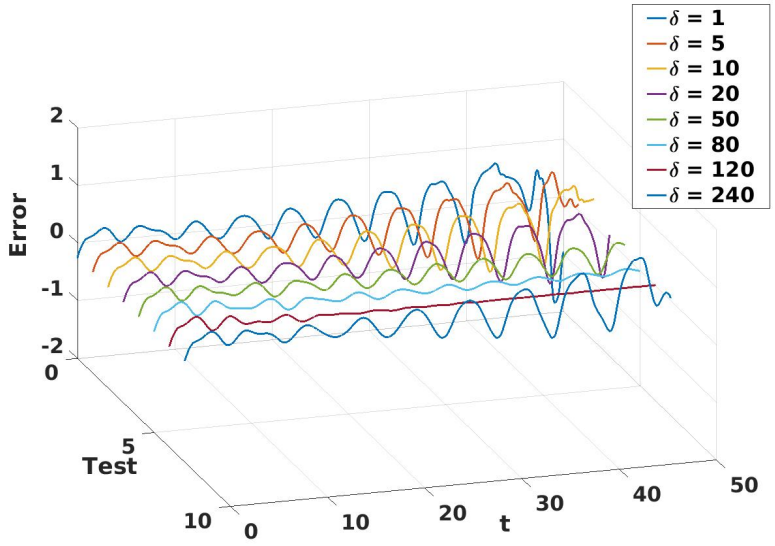

Figure 9: Tuning δ for G = 1.5.

which provides remarkable reduction of the angular velocity oscillations, with decreasing performance when increasing disturbance frequency.

Next, the Individual Pitch Repetitive Control (sketched in Fig. 15) is applied to the reduction of vibratory flap bending moment due to wind shear (Fig. 5 depicts the corresponding flap motion). Controlling this load, fatigue-life of blades and fixed structure components can be extended. A steady stable value for angular velocity is assured by application of a PI controller with proportional gain $P = -0.018$ and integral gain $I = -0.0014$. In Fig. 15 the angles θ_{ipc} are the portion of control input due to IPC, whereas θ_{cpc} represents the collective part. Final

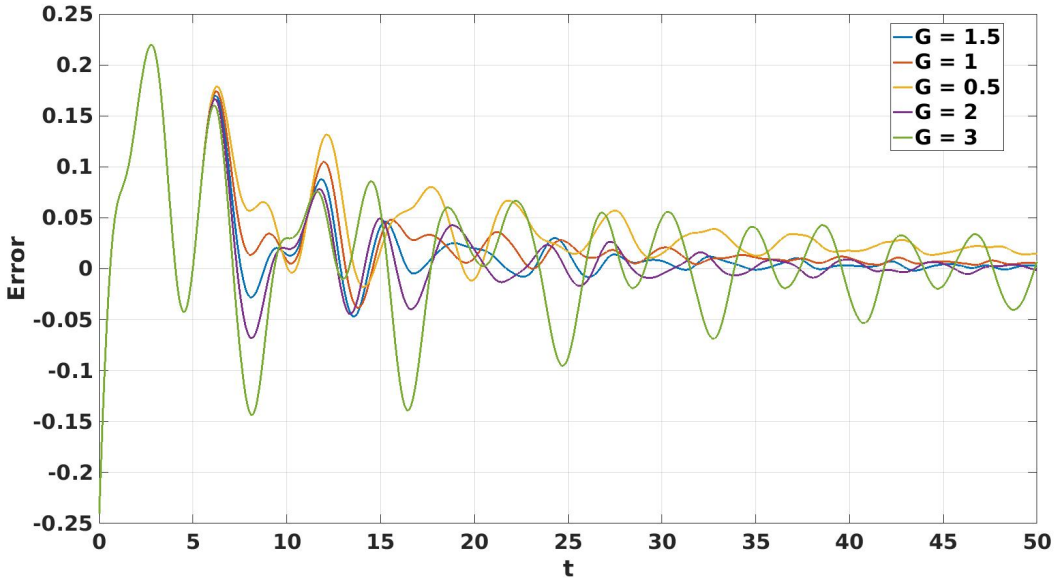

Figure 10: Tuning G for $\delta = 120$ samples.

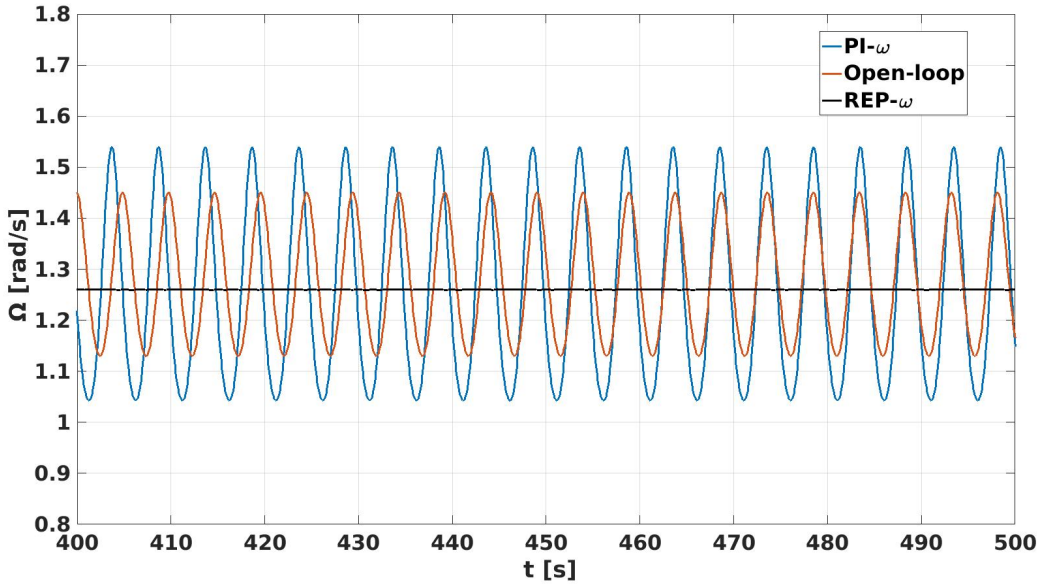

Figure 11: Effects of $1/rev$ external disturbance on open-loop and controlled responses.

control signal θ_{tot} is the sum of IPC and CPC angles, so three different torques are obtained through a central control which sums the two contributions (note that, in the IPC feedback loop, the gain $P = -0.0005$ is also present).

Also in this case, a tuning procedure similar to that described for CPC repetitive is carried out for setting the repetitive parameters (see Eq. (7)). As a result, the value $G = 1$ and the shift factor $\delta = 280°$ are identified. The error $e_j(k+1)$ is considered equal to the difference with respect to the mean nominal flapping moment value obtained from a previous analysis. The performance of the proposed repetitive controller is shown in Figs. 16-19 where its outcomes are compared with those determined by application of both an angular velocity PI collective

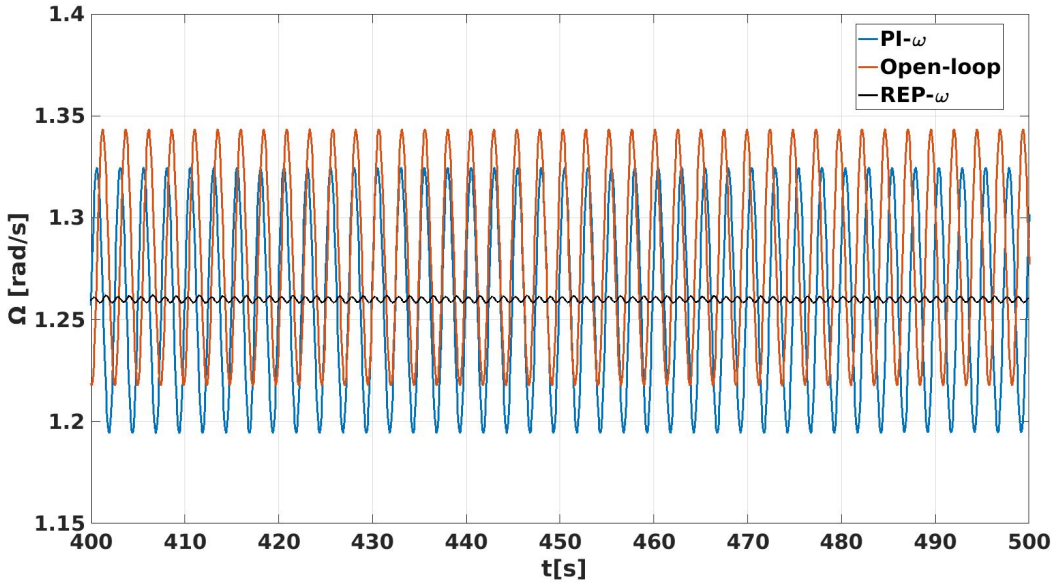

Figure 12: Effects of $2/rev$ external disturbance on open-loop and controlled responses.

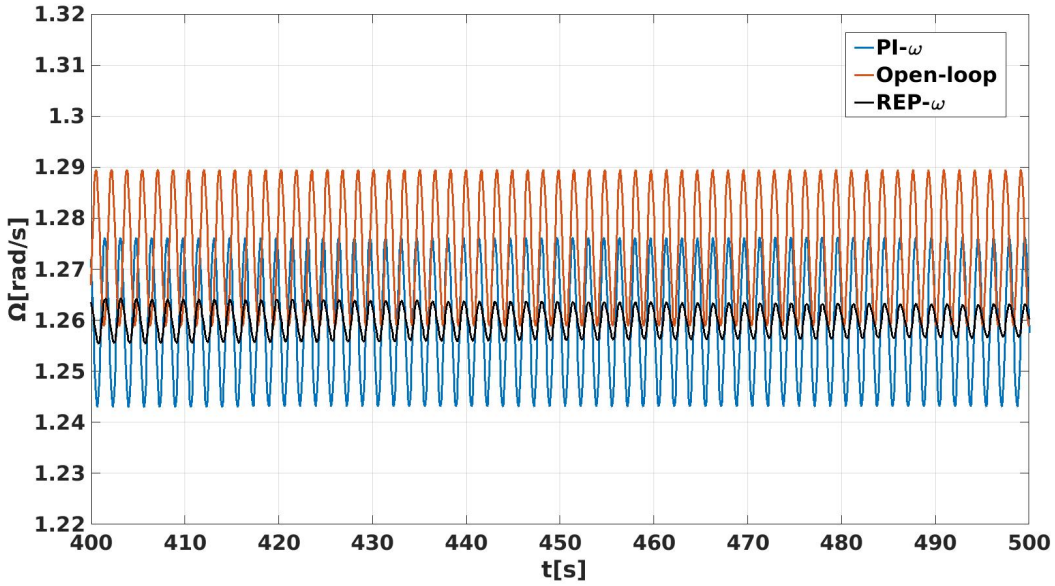

Figure 13: Effects of $3/rev$ external disturbance on open-loop and controlled responses.

controller (PI_ω) and an individual PI flap bending moment controller (PI_ω-$PI_{M_{flap}}$).

With application of the PI_ω controller , a steady state(blue curves in) value of angular velocity is reached (see Fig. 18), whereas flap bending moment and flap degree of freedom present undesired periodic behavior (blue curves in Figs. 16-17). The application of the PI_ω-$PI_{M_{flap}}$ controller provides reduced flapping moment and motion oscillations (of about -22%, as indicated by the red curves in Figs. 16-17). It assures the achievement of the nominal angular velocity, as well. Instead, with the application of the repetitive IPC the flapping moment and motion oscillations are strongly reduced (of about -94%, as indicated by the black curves in Figs. 16-17)). Also in this case the rotor nominal angular speed is achieved, demonstrating that

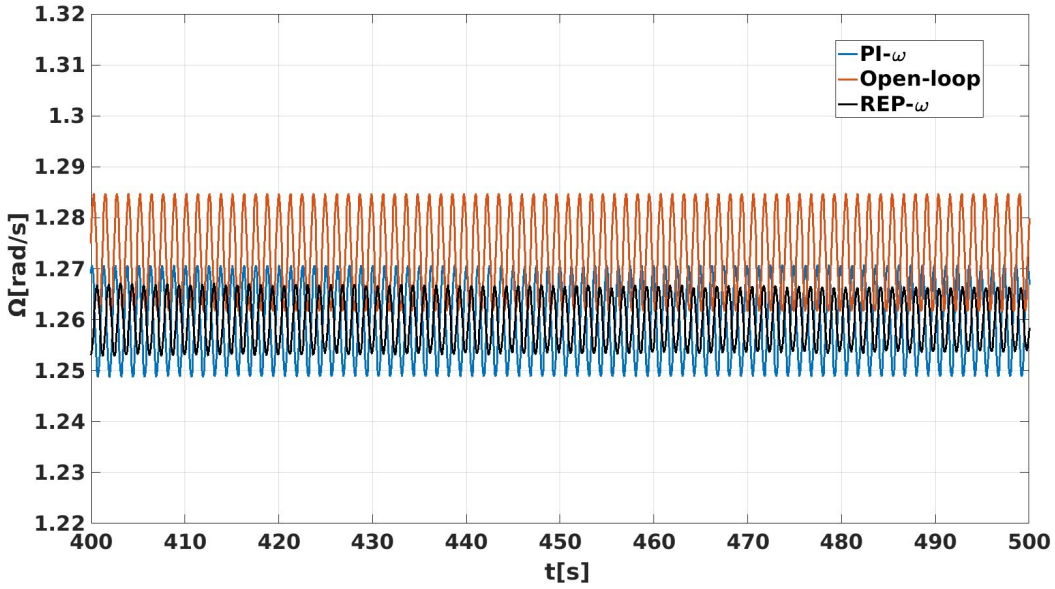

Figure 14: Effects of $4/rev$ external disturbance on open-loop and controlled responses.

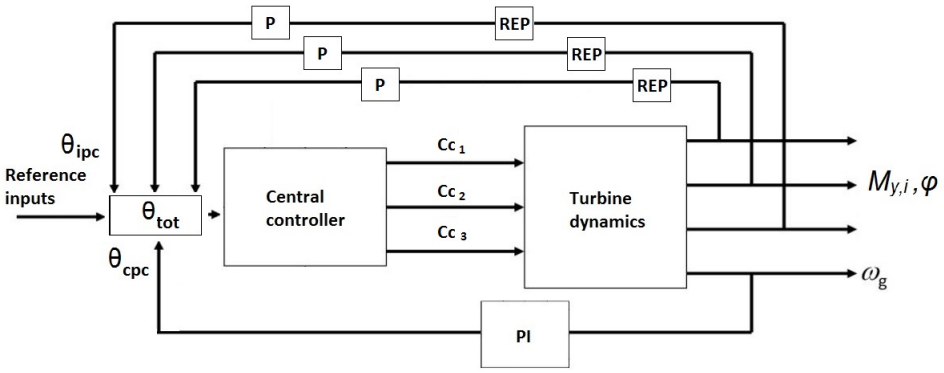

Figure 15: IPC flap motion control scheme.

no adverse interaction between PI-ω controller and IPC repetitive controller arises.

Furthermore, Fig. 19 depicts the FFT of the flap bending moment. Three peaks corresponding to the main harmonic components are shown. It is possible to observe that the $1/rev$, $2/rev$, $3/rev$ harmonic components (corresponding to 0.2 Hz, 0.4 Hz and 0.6 Hz) are reduced: 92% of reduction is achieved for the $1/rev$ component, while 63% of reduction is obtained for the $2/rev$ one.

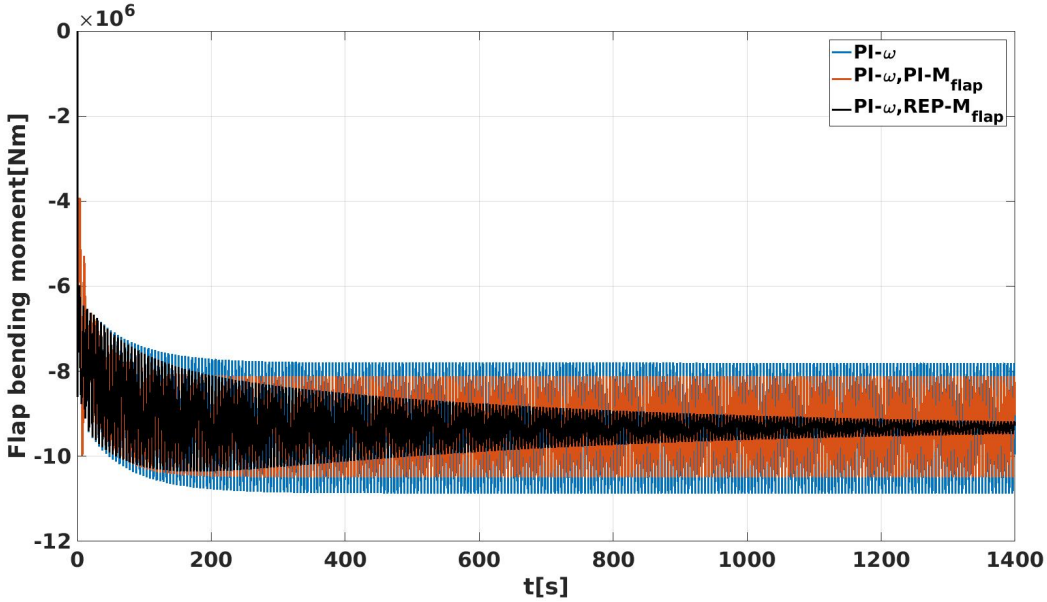

Figure 16: Bending moment for open-loop and controlled HAWT.

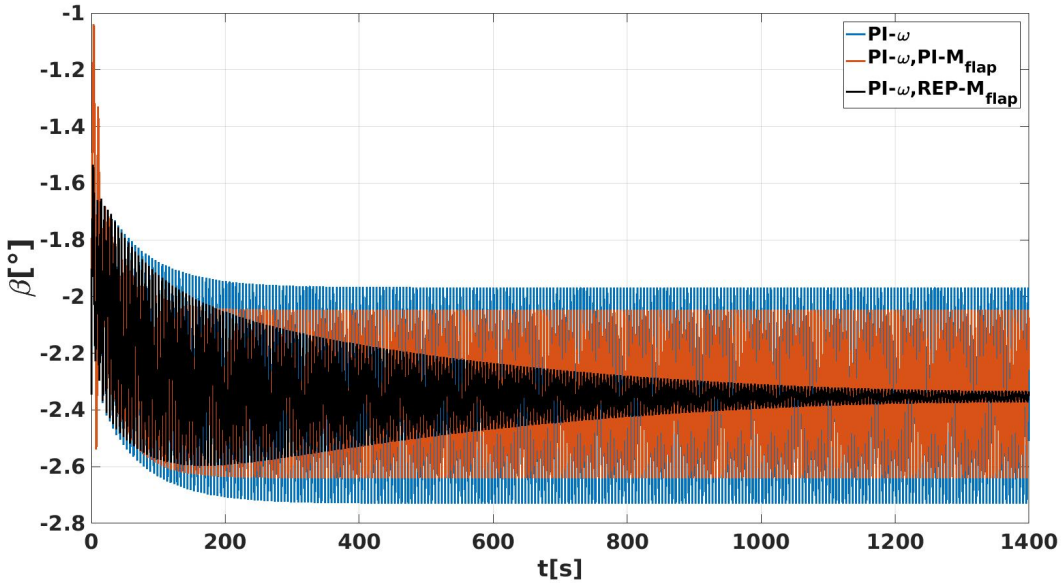

Figure 17: Flap angle for open-loop and controlled HAWT.

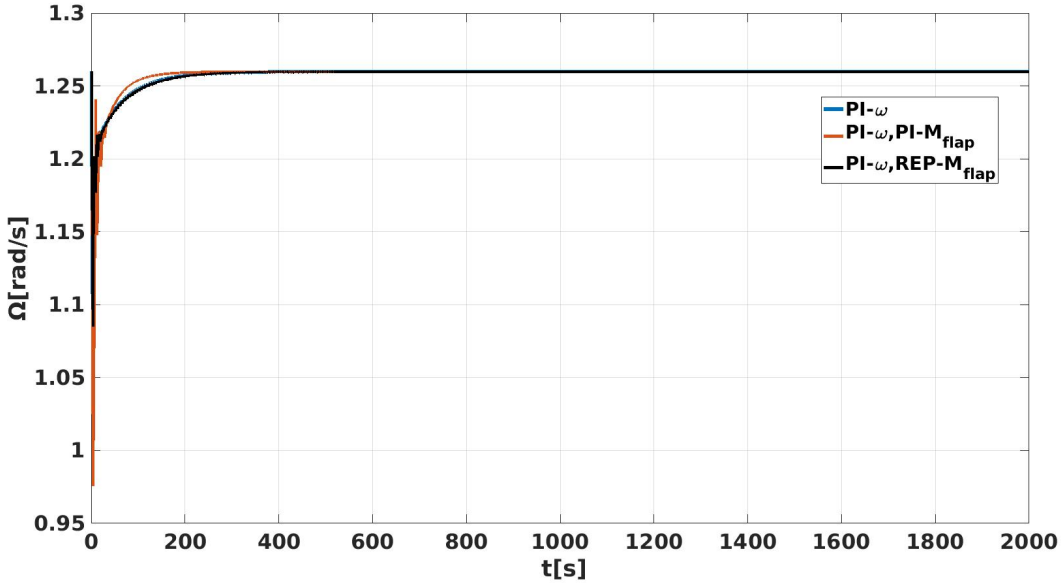

Figure 18: Angular velocity for open-loop and controlled HAWT.

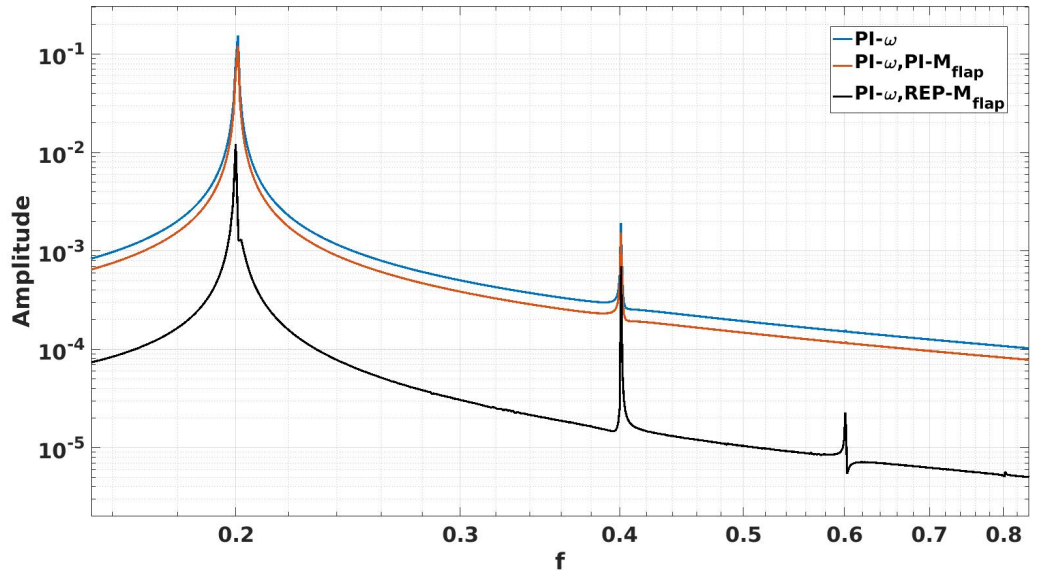

Figure 19: FFT of bending moment for open-loop and controlled HAWT.

5 CONCLUSIONS

In this paper, a nonlinear differential aeroelastic model for three-bladed horizontal axis wind turbine is developed and applied for control purposes. The model is obtained through the Euler-Lagrange formulation, whereas the aerodynamic loads are obtained using a quasi-steady strip theory. Wind shear effects are considered, such that periodic components are forced to turbine angular velocity, flap bending moment and flap displacement. A Repetitive-PI collective pitch controller has been tested for angular velocity control, under the effect of periodic disturbances of the wind. In addition a repetitive individual pitch controller has been applied for vibratory flapping moment induced by wind shear, combined with a PI collective control for angular velocity. For both problems, the proposed repetitive controller has demonstrated to be very successful, remarkably more effective than classical PI controller: it is capable of rejecting the periodic perturbations introduced, while tracking the nominal angular velocity. All the harmonic components of the flapping moment have been reduced by application of the repetitive individual pitch controller.

6 REFERENCES

[1] Feinberg, S. (2011). Wind turbine prices fall to their lowest in recent years. *Bloomberg New Energy Finance*.

[2] Smith, K., Randall, G., Malcolm, D., et al. (2002). Evaluation of wind shear patterns at midwest wind energy facilities. In *American Wind Energy Association (AWEA) WINDPOWER 2002 Conference*.

[3] Rehman, S. and Al-Abbadi, N. M. (2005). Wind shear coefficients and their effect on energy production. *Energy Conversion and Management*, 46(15), 2578–2591.

[4] Rehman, S. and Al-Abbadi, N. M. (2008). Wind shear coefficient, turbulence intensity and wind power potential assessment for dhulom, saudi arabia. *Renewable Energy*, 33(12), 2653–2660.

[5] Shen, X., Zhu, X., and Du, Z. (2011). Wind turbine aerodynamics and loads control in wind shear flow. *Energy*, 36(3), 1424–1434.

[6] Yang, Z., Li, Y., and Seem, J. E. (2011). Individual pitch control for wind turbine load reduction including wake interaction. In *Proceedings of the 2011 American Control Conference*. IEEE, pp. 5207–5212.

[7] Manwell, J. F., McGowan, J. G., and Rogers, A. L. (2010). *Wind energy explained: theory, design and application*. John Wiley & Sons.

[8] Bianchi, F. D., De Battista, H., and Mantz, R. J. (2006). *Wind turbine control systems: principles, modelling and gain scheduling design*. Springer Science & Business Media.

[9] Spera, D. A. (1994). Wind turbine technology.

[10] Laks, J. H., Pao, L. Y., and Wright, A. D. (2009). Control of wind turbines: Past, present, and future. In *American Control Conference, 2009. ACC'09.* IEEE, pp. 2096–2103.

[11] Ringwood, J. V. and Simani, S. (2015). Overview of modelling and control strategies for wind turbines and wave energy devices: Comparisons and contrasts. *Annual Reviews in Control*, 40, 27–49.

[12] Bossanyi, E. (2003). Individual blade pitch control for load reduction. *Wind energy*, 6(2), 119–128.

[13] Larsen, T. J., Madsen, H. A., and Thomsen, K. (2005). Active load reduction using individual pitch, based on local blade flow measurements. *Wind Energy*, 8(1), 67–80.

[14] Olsen, T., Lang, E., Hansen, A., et al. (2004). Low wind speed turbine project conceptual design study: Advanced independent pitch control; july 30, 2002–july 31, 2004 (revised). Tech. rep., National Renewable Energy Lab., Golden, CO (US).

[15] Hand, M., Wright, A., Fingersh, L., et al. (2006). Advanced wind turbine controllers attenuate loads when upwind velocity measurements are inputs. In *44th AIAA Aerospace Sciences Meeting and Exhibit*. p. 603.

[16] Hand, M. M. (2003). *Mitigation of wind turbine/vortex interaction using disturbance accommodating control*. National Renewable Energy Laboratory Boulder, CO.

[17] Stol, K. A. (2003). Disturbance tracking and blade load control of wind turbines in variable-speed operation. In *ASME 2003 Wind Energy Symposium*. American Society of Mechanical Engineers, pp. 317–323.

[18] Wright, A. D. (2004). *Modern control design for flexible wind turbines*. National Renewable Energy Laboratory Golden, CO.

[19] Wright, A. D. and Fingersh, L. (2008). Advanced control design for wind turbines; part i: control design, implementation, and initial tests. Tech. rep., National Renewable Energy Laboratory (NREL), Golden, CO.

[20] Bossanyi, E., Fleming, P., and Wright, A. (2012). Field test results with individual pitch control on the nrel cart3 wind turbine. In *50th AIAA Aerospace Sciences Meeting including the New Horizons Forum and Aerospace Exposition*. p. 1019.

[21] Rezaei, V. and Johnson, K. E. (2013). Robust fault tolerant pitch control of wind turbines. In *Decision and Control (CDC), 2013 IEEE 52nd Annual Conference on*. IEEE, pp. 391–396.

[22] Schlipf, D., Schlipf, D. J., and Kühn, M. (2013). Nonlinear model predictive control of wind turbines using lidar. *Wind Energy*, 16(7), 1107–1129.

[23] Gros, S. (2013). An economic nmpc formulation for wind turbine control. In *Decision and Control (CDC), 2013 IEEE 52nd Annual Conference on*. IEEE, pp. 1001–1006.

[24] Friis, J., Nielsen, E., Bonding, J., et al. (2011). Repetitive model predictive approach to individual pitch control of wind turbines. In *Decision and Control and European Control Conference (CDC-ECC), 2011 50th IEEE Conference on*. IEEE, pp. 3664–3670.

[25] Hosseini, H. and Kalantar, M. (2012). Repetitive control scheme for an ecs to improve power quality of grid connected wind farms using svm. In *Smart Grids (ICSG), 2012 2nd Iranian Conference on*. IEEE, pp. 1–7.

[26] Houtzager, I., van Wingerden, J.-W., and Verhaegen, M. (2013). Rejection of periodic wind disturbances on a smart rotor test section using lifted repetitive control. *IEEE Transactions on Control Systems Technology*, 21(2), 347–359.

[27] Fratini, R., Santini, R., Serafini, J., et al. (2016). A spatial repetitive controller applied to an aeroelastic model for wind turbines. *World Academy of Science, Engineering and Technology, International Journal of Mechanical, Aerospace, Industrial, Mechatronic and Manufacturing Engineering*, 10(9), 1615–1623.

[28] Greenberg, J. M. (1947). Airfoil in sinusoidal motion in a pulsating stream.

[29] Theodorsen, T. (1949). General theory of aerodynamic instability and the mechanism of flutter. Tech. Rep. TR-496, NACA.

[30] Hodges, D. and ORMISTON, R. (1973). Stability of elastic bending and torsion of uniform cantilevered rotor blades in hover. In *14th Structures, Structural Dynamics, and Materials Conference*. p. 405.

7 COPYRIGHT STATEMENT